*magnetochemistry*

MDPI

*Article*

# Magnetic Field Effects on Chemical Reaction of Power-Law Fluid over an Axisymmetric Stretched Sheet

**Mohammad Yaghoub Abdollahzadeh Jamalabadi**

Department of Mechanical, Robotics and Energy Engineering, Dongguk University, Seoul 04672, Korea; abdollahzadeh@dongguk.edu

Received: 9 May 2019; Accepted: 2 September 2019; Published: 8 October 2019


**Abstract:** Numerical investigation of the effects of magnetic field strength, thermal radiation, Joule heating, and viscous heating on a forced convective flow of a non-Newtonian, incompressible power-law fluid in an axisymmetric stretching sheet with variable temperature wall is accomplished. The power-law shear-thinning viscosity-shear rate model for the anisotropic solutions and the Rosseland approximation for the thermal radiation through a highly absorbing medium is considered. The temperature-dependent heat sources, Joule heating, and viscous heating are considered to be the source terms in the energy balance. The non-dimensional boundary-layer equations are solved numerically in terms of similarity variable. A parameter study on the boundary value of chemical reaction and Nusselt number is performed as a function of thermal radiation parameter, Brinkman number, Prandtl number, Hartmann number, power-law index, heat source coefficient, Brownian parameter, thermophoresis parameter, and the chemical reaction parameter. The results show that the chemical reaction parameter has an increasing effect on the chemical reaction boundary while the magnetic, thermophoresis, and Brownian effects decrease the rate of the chemical reaction at the boundary.

**Keywords:** thermal radiation; forced convection; viscous dissipation; power-law index; stretching sheet; thermophoresis effect; Brownian effect; chemical reaction

## 1. Introduction

Flow past a stretching plate has been a topic of the research for around half a century [1]. One of the aspects of this flow is its effect on the heat and mass transfer [2]. The forced convective heat transfer on a stretching sheet with injection, suction, and blowing with variable temperature are studied by Grubka and Bobba [3]. They showed the thermodynamic aspects of the problem is affected significantly by the flow characteristics. The application of this problem is in the industry of the wire drawing [4] manufacturing of hot rolling glass fiber [5], drawing plastic sheet [6], cooling and drying of papers [7], melting of polymers [8], etc. The temperature field in a flow over a stretching plate with a uniform heat flux [6] and with variable heat flux [8] including the distribution of heat transfer reveals the effect of flux distribution on the thermal balance in the volume. Hooshmand et al. solved the flow past a stretching plate and the solution obtained reveals that for constant surface temperature the skin friction coefficient increases with the Reynolds number [9]. The research also contains the effect of thermal radiation on a stretching plate [9,10]. Flow and heat transfer of a fluid through a porous medium over a stretching surface with internal heat generation/absorption and suction/blowing is studied by Cortell [11].

Transient flow is solved analytically for the case of unsteady boundary-layer flows caused by an impulsively stretching plate [12]. There is a great difference between the solution of Liao [12]

and the simple model in boundary-layer flow derived by Mehmood [13]. Hydro-magnetic effects adjacent [14] to a stretching vertical sheet and inside the boundary-layer flow [15] was studied by researchers. Furthermore, the geometry is varied from plate [1,9,12] to cylinder [15–18]. The effect of magnetohydrodynamics (MHD) on the flow and heat transfer due to a stretching cylinder was studied by Ishak et al. [19]. Existence of a solution and prior bounds for steady stagnation flow toward a stretching cylinder by Mastroberardino and Paullet [20] and Aligned and non-aligned radial stagnation flow on a stretching cylinder by Weidman and Ali [21] showed that the concentration of the flow can increase the heat transfer locally.

Stretching of the cylinder can cause slip effects [22] and vacillation [23]. Those effects can be controlled by hydro-magnetic effects [24]. The MHD control is used in various applications such as two-phase flow-induced vibrations in the vertical heated upward flow [25–27], hemodynamic [28–30], and polymer applications [31–33]. The problem is solved in Cartesian [34–41] and cylindrical coordinates [42,43]. In the International Plastics Handbook [44] and Mechanical and Thermophysical Properties of Polymer Liquid Crystals [45] thermal and physical properties of polymers are given and used for the current study. The Rosseland approximation [46].

Previous work on MHD flow [47] with radiation heat transfer [10,48–50] with models [51,52] and methods [53,54], in various media [55–73].

The media can be categorized as porous [55], convective [56], microchannel [57], square cavity [58], gravity flows [59], gravity currents [60], suspensions [61], shear-thinning [62], porous gravity currents [63], power-law gravity currents [64], vertically graded porous media [65], confining boundaries [66], gravity porous media [67], propagative [68–70], pressure-dependent [71], rheological [72], and varying cross-sections and inclinations [73]. The literature is very broad but few papers consider all the effects in one study. The importance of this work is in considering all those parameters in one problem.

Hayat et al. solved the Jeffrey fluid problem with Cattaneo–Christov heat flux (a combination of transient thermal and velocity), double stratification, and chemical reaction effects [74]. Modified Fourier's law (parabolic heat conduction) showed decreases in temperature at higher thermal relaxation. MHD effects on homogeneous (first-order kinetics $A \rightarrow B, \quad rate = k_2 C_a,$) and heterogeneous (cubic autocatalytic kinetics $A + 2B \rightarrow 3B, \quad rate = k_1 C_a C_b^2,$) reactions have been studied by Khan et al. [75]. They showed that homogeneous reactions are governed by first-order kinetics, but the effect of MHD on boundary chemical flux was not considered. MHD effects on mixed convective flow caused by a rotating disk were studied by Hayat et al. [76] without the chemical reaction. The impacts of Joule heating, Brownian model, Buongiorno model, and non-linear thermal radiation on Walter-B fluid is addressed in [77]. Khan et al. [77] ignored the effect of a self-sustained chemical reaction and the reaction caused by Brownian diffusion and thermophoresis diffusion effects. Rashid [78] studied the flow of magnetite $Fe_3O_4$ nano liquid over a stretching sheet. Heat source/sink, non-linear radiation, velocity, and thermal slip aspects were considered by them, but chemical reactions are ignored.

Considering all the above, the goal of the present article was to investigate the MHD effects in a steady-state fully developed non-Newtonian incompressible flow over an axisymmetric stretching sheet and the Rosseland approximation model in the chemical reactive environment where the Brownian and thermophoresis effects affect the transport of diluted species. Furthermore, the chemical reaction will affect the thermal balance of the system with released heat and with heating at a specific rate. In the next section, the complex nature of the governing equations describing the flows of the system are presented. Similarity transformation is used to reduce the governing equations of the problem into a system of non-linear ordinary differential equations. The resulting system of coupled equations are solved and discussed in the last section. A parameter study on chemical reactions including thermal radiation parameter, Brinkman number, Prandtl number, Hartmann number, power-law index, heat source coefficient, Brownian parameter, thermophoresis parameter, and chemical reaction parameter is performed. Numerical values are expressed in terms of graphs to

investigate the influence of various flow, controlling parameters such as radiation parameter, Prandtl number, magnetic parameter, chemical parameter, and power-law parameter. The conclusions are presented in the conclusion section.

## 2. Governing Equations

To study the MHD effects on chemical reaction near an infinitely radially stretching sheet, an axisymmetric two-dimensional sketch as shown in Figure 1 is well considered. The fluid is considered to be an incompressible liquid. To understand the effect of melting, non-Newtonian models are considered. As exemplified, the fluid in contact with the surface of the non-permeable stretching sheet will travel along with the sheet without any slippage.

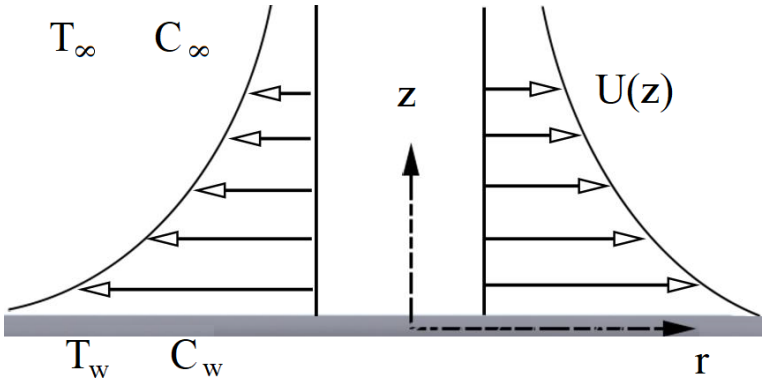


**Figure 1.** Schematic representation of the considered problem.

In cylindrical coordinates the continuity is:

$$\frac{\partial v}{\partial r} + \frac{v}{r} + \frac{\partial u}{\partial z} = 0 \tag{1}$$

and the momentum equation is:

$$\rho\left(v\frac{\partial v}{\partial r} + u\frac{\partial v}{\partial z}\right) = \frac{\partial}{\partial z}\left(K\left|\frac{\partial v}{\partial z}\right|^{n-1}\frac{\partial v}{\partial z}\right) - \sigma B^2 v \tag{2}$$

where power-law indexes for common materials are presented in Table 1.

**Table 1.** power-law indexes.

| Material | *n* |
|---|---|
| high density polyethylene | 0.41 |
| low density polyethylene | 0.39 |
| polyamide | 0.66 |
| polycarbonate | 0.98 |
| polypropylene | 0.38 |
| polystyrene | 0.28 |
| polyvinyl chloride | 0.26 |

The energy equation for thermal balance is:

$$\rho C_p\left(v\frac{\partial T}{\partial r} + u\frac{\partial T}{\partial z}\right) = \frac{\partial}{\partial z}\left(k\frac{\partial T}{\partial z} - \frac{\partial q_r}{\partial z}\right) + K\left|\frac{\partial v}{\partial z}\right|^{n+1} + \sigma B^2 v^2 + Q(T - T_{ref}) + \rho C_p D_B \frac{\partial C}{\partial z}\frac{\partial T}{\partial z} + \rho C_p \frac{D_T}{D_\infty}\left(\frac{\partial T}{\partial z}\right)^2 \tag{3}$$

where $q_r$ is modeled by Rosseland approximation:

$$q_r = -\frac{4\sigma*}{3\chi}\frac{\partial T^4}{\partial z}, \tag{4}$$

For the optically thick medium with the optical thickness ($\chi \times r$) greater than 3 and the boundary layer [38] and using a linear approximation for temperature ($T^4 \approx 4T_\infty^3 T - 3T_\infty^4$) the energy balance is:

$$\rho C_p\left(v\frac{\partial T}{\partial r} + u\frac{\partial T}{\partial z}\right) = \frac{\partial}{\partial z}\left(k\frac{\partial T}{\partial z} + \frac{4\sigma^*}{3\chi}\frac{\partial\left(n^2T^4\right)}{\partial z}\right) + K\left|\frac{\partial v}{\partial z}\right|^{n+1} + \sigma B^2v^2 + Q(T - T_\infty) + \rho C_p D_B\frac{\partial C}{\partial z}\frac{\partial T}{\partial z} + \rho C_p\frac{D_T}{D_\infty}\left(\frac{\partial T}{\partial z}\right)^2 \tag{5}$$

The governing boundary-layer equations for mass transfer is

$$v\frac{\partial C}{\partial r} + u\frac{\partial C}{\partial z} = \frac{\partial}{\partial z}\left(D_B\frac{\partial C}{\partial z}\right) + \frac{\partial}{\partial z}\left(\frac{D_T}{D_\infty}\frac{\partial T}{\partial z}\right) - k_1\left(C - C_\infty\right) \tag{6}$$

boundary conditions are:

$$v\left(z = 0\right) = cr^{1/3} \tag{7}$$

where shrink rates for common plastics are presented in Table 2.

$$v\left(z = \infty\right) = 0 \tag{8}$$

$$u\left(z = 0\right) = 0 \tag{9}$$

$$T\left(z = 0\right) = T_w \tag{10}$$

$$T\left(z = \infty\right) = T_\infty \tag{11}$$

$$C\left(z = 0\right) = C_w \tag{12}$$

$$C\left(z = \infty\right) = C_\infty \tag{13}$$

**Table 2.** Shrink rates for common plastics.

| Material | Shrink Rate (/in/in) |
|---|---|
| ABS | 0.005–0.007 |
| acetal | 0.018–0.025 |
| acrylic | 0.002–0.008 |
| nylon 6 | 0.006–0.014 |
| nylon 66 | 0.012–0.018 |
| polycarbonate | 0.005–0.007 |
| PET | 0.005–0.012 |
| polyethylene | 0.015–0.050 |
| polypropylene | 0.010–0.025 |
| PP (30% glass) | 0.004–0.0045 |
| polystyrene | 0.002–0.006 |
| PS (30% glass) | 0.0005–0.0010 |
| PVC | 0.003–0.0008 |

The governing equations can be reduced to ordinary differential equations, using the similarity transformation. The equivalent stream formulations ($v = -\frac{1}{r}\frac{\partial \psi}{\partial z}, u = \frac{1}{r}\frac{\partial \psi}{\partial r}$) of momentum and energy equations by the dimensionless temperature definition ($\theta = \frac{T-T_\infty}{T_w-T_\infty}$) are:

$$\frac{1}{r^2}\frac{\partial^2\psi}{\partial r\partial z}\frac{\partial \psi}{\partial z} - \frac{1}{r^3}\left(\frac{\partial \psi}{\partial z}\right)^2 - \frac{1}{r^2}\frac{\partial \psi}{\partial r}\frac{\partial^2\psi}{\partial z^2} = \frac{K}{\rho}\left(-\frac{1}{r}\right)^n \frac{\partial}{\partial z}\left(\left|\frac{\partial^2\psi}{\partial z^2}\right|^{n-1}\frac{\partial^2\psi}{\partial z^2}\right) + \frac{\sigma B^2}{\rho r}\frac{\partial \psi}{\partial z} \tag{14}$$

$$\frac{1}{r}\frac{\partial \psi}{\partial r}\frac{\partial \theta}{\partial z} - \frac{1}{r}\frac{\partial \psi}{\partial z}\frac{\partial \theta}{\partial r} = \frac{k}{\rho C_p}\frac{\partial^2\theta}{\partial z^2}(1+N_R) + \frac{K}{\rho C_p\left(T_w-T_\infty\right)}\left|-\frac{1}{r}\frac{\partial^2\psi}{\partial z^2}\right|^{n+1} + \frac{\sigma B^2}{\rho C_p\left(T_w-T_\infty\right)r^2}\left(\frac{\partial \psi}{\partial z}\right)^2 + \frac{Q}{\rho C_p}\theta + D_B\frac{\partial \phi}{\partial z}\frac{\partial \theta}{\partial z} + \frac{D_T}{D_\infty}\left(\frac{\partial \theta}{\partial z}\right)^2 \tag{15}$$

where

$$k_R = \frac{\sigma^* n^2\left(T_w-T_\infty\right)^3}{3k\chi} \tag{16}$$

Furthermore, the mass transfer equation by considering the dimensionless concentration definition ($\phi = \frac{C-C_\infty}{C_w-C_\infty}$) is:

$$\frac{1}{r}\frac{\partial \psi}{\partial r}\frac{\partial \phi}{\partial z} - \frac{1}{r}\frac{\partial \psi}{\partial z}\frac{\partial \phi}{\partial r} = \frac{\partial}{\partial z}\left(D_B\frac{\partial \phi}{\partial z}\right) + \frac{\partial}{\partial z}\left(\frac{D_T}{D_\infty}\frac{\partial \theta}{\partial z}\right) - k_1\phi \tag{17}$$

The $r$ component of velocity is assumed to have the following profile:

$$v = cr^{1/3}f'(\eta) \tag{18}$$

where $\eta$ is

$$\eta = \left(\frac{5\rho c^{2-n}}{3Kn}\right)^{\frac{1}{n+1}} r^{1/3}z \tag{19}$$

and stream function is

$$\psi = \beta r^{\frac{5}{3}}f(\eta) \tag{20}$$

the resulted axial velocity component is:

$$u = -\sqrt[n+1]{\frac{3Knc^{2n-1}}{5\rho}}\frac{r^{-1/3}\left(5f-\eta f'\right)}{3} \tag{21}$$

the magnetic field distribution is:

$$B = B_0 r^{-1/3} \tag{22}$$

the heat source coefficient is:

$$Q = Q_0 r^{-2/3} \tag{23}$$

Since the non-dimensional momentum and energy equations are:

$$\left|f''\right|^{n-1}f''' + ff'' - \left(\frac{f'^2+3Ha^2f'}{5}\right) = 0 \tag{24}$$

$$(1+N_R)\theta'' + \frac{5\mathrm{Pr}}{3}f\theta' + Br\left|f''\right|^{n+1} + Ha^2f'^2 + \hat{Q}\theta + N_b\phi'\theta' + N_t\left(\theta'\right)^2 = 0, \tag{25}$$

$$\phi'' + Scf\phi' - \gamma\phi + \frac{N_t}{N_b}\theta'' = 0, \tag{26}$$

with boundary conditions of:

$$f(0) = 0 \tag{27}$$

$$f'(0) = 1 \tag{28}$$

$$\lim_{\eta\to\infty} \quad f'(\eta) = 0 \tag{29}$$

$$\theta\,(z = 0) = 1 \tag{30}$$

$$\lim_{\eta\to\infty} \quad \theta(\eta) = 0 \tag{31}$$

$$\phi\,(z = 0) = 1 \tag{32}$$

$$\lim_{\eta\to\infty} \quad \phi(\eta) = 0 \tag{33}$$

The velocity, temperature, and concentration profiles are obtained by solving Equations (24)–(26) with boundary conditions (27)–(33) by assigning numerical values to the parameter encounter in the problem. Dimensionless parameters are as follow:

- heat source is:

$$\hat{Q} = \frac{Q_0}{k}\sqrt[n+1]{\frac{9K^2n^2c^{2n-4}}{25\rho^2}} \tag{34}$$

- The Prandtl number is:

$$\mathrm{Pr} = \frac{C_p}{k}\sqrt[n+1]{\frac{9\rho^{n-1}K^2n^2c^{3n-3}}{25}} \tag{35}$$

- The Péclet number is

$$Pe = \rho K c^n \alpha^{n+1} \tag{36}$$

- Hartman number is:

$$Ha = B_0\sqrt{\frac{\sigma}{\rho c}} \tag{37}$$

- The Brinkman number is:

$$Br = \frac{Kc^{n+1}\alpha^{n-1}}{k\Delta T} \tag{38}$$

- The Schmidt number (Sc) is a dimensionless number defined as the ratio of momentum diffusivity (kinematic viscosity) and mass diffusivity:

$$Sc = v/D_B \tag{39}$$

- Lewis number is a dimensionless number which is the ratio of thermal diffusivity to mass diffusivity, $\alpha/D_B$, (or) Schmidt number to Prandtl number

$$Le = Sc/Pr \tag{40}$$

- Brownian motion parameter is

$$N_b = \frac{D_B(C_\infty - C_w)}{v} \tag{41}$$

- thermophoresis parameter is

$$N_t = \frac{D_T(T_\infty - T_w)}{vT_\infty} \tag{42}$$

- chemical reaction parameter is

$$\gamma = \frac{k_1 c D_B(C_\infty - C_w)}{v} \tag{43}$$

## 3. Results and Discussion

The non-linear ordinary differential Equations (24)–(26) with boundary conditions (27)–(33) have been solved by implementing the Runge–Kutta–Fehlberg fourth–fifth-order method with shooting technique. The work presents a study on the physical aspects of MHD on the chemical reactions on non-Newtonian fluid flow over stretching surface which has a significant role in food processing, polymer manufacturing, chemical engineering industries, and metallurgy. The mathematical modeling of the physical problem, which is coupled heat and mass transfer problem, include the non-linear set of partial differential equations. The coupled non-linear equations are solved for different values of parameters. To validate the compatibility of the computed solution, Table 3 is developed to compare the present work with past works, with which this comparison shows excellent agreement. The schematic details of the compared model are the same as the current problem, which is shown in Figure 1.

**Table 3.** Comparison of the $f$ between the present results and those obtained previously [51] for the special case of, $Ha = 0$, $n = 0$, and non-linear stretching ($m = -1/3$).

| | **Present Work** | **Khan et al. [51]** |
|---|---|---|
| $f''$ | 1.17 | 1.173721 |
| $NuRe^{\frac{-1}{n+1}}$ | 0.787 | 0.789183 |

A set of non-linear ordinary differential equations are of third order in $f$, second order in $\theta$ and $\phi$, and are first reduced into a system of simultaneous ordinary equations. The system of ODE is in the form of

$$Y' = g(Y) \tag{44}$$

where

$$Y = \begin{bmatrix} y_1 \\ y_2 \\ y_3 \\ y_4 \\ y_5 \\ y_6 \\ y_7 \end{bmatrix} = \begin{bmatrix} f \\ f' \\ f'' \\ \theta \\ \theta' \\ \phi \\ \phi' \end{bmatrix} \tag{45}$$

and the function g is

$$g(Y) = \begin{bmatrix} y_2 \\ y_3 \\ -y_1^{2-n} y_3 + y_1^{1-n}(y_2^2/5 + 3/5Ha^2 y_2)y_5 \\ \frac{5/3Pry_1y_5 + Br|y_3|^{n+1} + Ha^2.y_2^2 + Qy_4 + N_t y_5^2 + N_b.y_5.y_7}{-1-NR} \\ y_7 \\ -Sc.y_1.y_7 + \gamma.y_6 - Nt/Nb\frac{5/3Pry_1y_5 + Br|y_3|^{n+1} + Ha^2.y_2^2 + Qy_4 + N_t y_5^2 + N_b.y_5.y_7}{-1-NR} \end{bmatrix} \tag{46}$$

Using trial and error or some scientific approach, one attempts to get as close to the boundary value as possible. The most essential step of this method is to choose the appropriate finite value for far-field boundary conditions. Here, infinity condition is taken at a large but finite value of $\eta$, where no considerable variations in velocity, temperature and so on occur. We run our bulk computations with the value at $\eta_{max} = 5$, which is sufficient to achieve far-field boundary conditions asymptotically for all values of the parameters considered. Figure 1 shows the schematic of the flow model where the $z$-axis represents the horizontal direction and the $r$-axis is normal to it. It is assumed that the sheet has an infinite radius and the surface is exposed to stretching by specific velocity. Before discussing the

results, first the results of the current problem are compared with earlier research. Table 3 presents a comparison of the $f$ between the present results and those obtained previously [51] for the special case of, $Ha = 0$, $n = 0$, and non-linear stretching ($m = -1/3$). That shows the results could be interpreted in perspective of previous studies and the working hypotheses. They are the same in geometry. Since the most important parameter is compared, and they are found to be in excellent agreement. Furthermore, the value of the local Nusselt number is compared for the case of $Pr = 1$ and $n = 0.5$, which shows that the current method underestimates that value, but they are generally in good agreement. Numerical values are expressed in terms of graphs to investigate the influence of the Hartmann number as well as the chemical reaction parameter, Brownian motion, and thermo-phoresis parameter. General results of solved parameters are plotted in Figures 2–4. Figures 2–4 demonstrate that with an increase in curvature of the cylinder we would have an increase in velocity, temperature, and concentration profiles, respectively. As shown in Figure 2 the $f'$ function decrease as the distance from the wall increases. The Figure is a plot of results obtained for $N_b = 0$, $N_t = 0$, $Ha = 0$, $Q = 0$, $Pr = 1$, $Br = 1$, $\gamma = 1$, $Sc = 1$. Radial velocity distributions show that the inside the boundary layer the velocity decrease gradually as a result of non-linear viscosity of the fluid. This is because an increase in Hartmann number will increase the intensity of body force, which acts as a blowing boundary condition at the stretching surface and hence tends to thicken the boundary layer. Figure 3 reveals the concentration distribution versus the non-dimensional distance. The Figure is a plot of results obtained for $N_b = 0$, $N_t = 0$, $Ha = 0$, $Q = 0$, $Pr = 1$, $Br = 1$, $\gamma = 1$, $Sc = 1$. It is observed that for increasing values of distance, the dimensionless concentration decreases, and the velocity boundary-layer thickness increases and decreases the temperature distribution. It is realized that an increase in the value of chemical reaction parameter decreases the concentration of species in the boundary layer, whereas the velocity and temperature of the fluid are not significant with an increase in chemical reaction parameter. Figure 4 exposes the temperature distribution versus the non-dimensional distance. The Figure is a plot of results obtained for $N_b = 0$, $N_t = 0$, $Ha = 0$, $Q = 0$, $Pr = 1$, $Br = 1$, $\gamma = 1$, $Sc = 1$. It is observed that for increasing values of distance, the dimensionless temperature decreases, and the velocity boundary-layer thickness increases and decreases the temperature distribution.

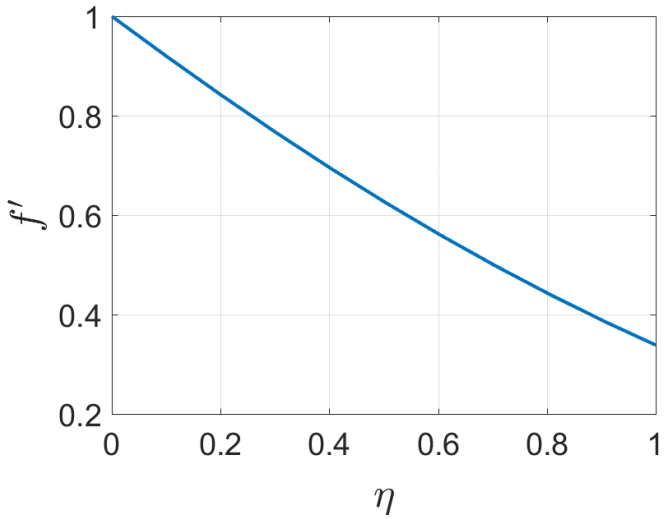


**Figure 2.** MHD Effects on velocity distribution.

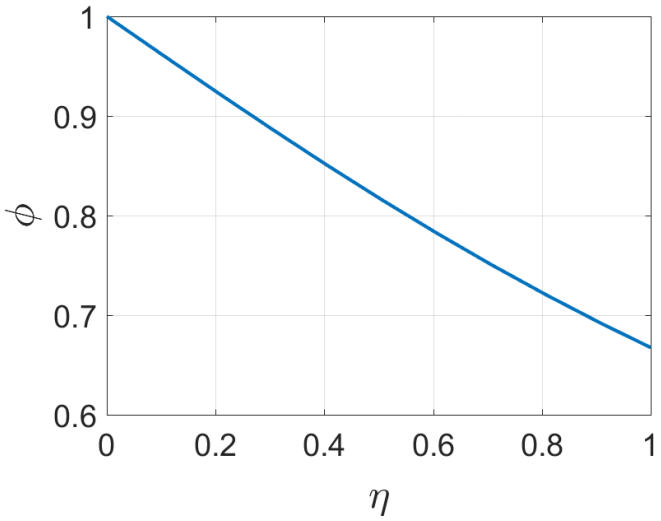


**Figure 3.** Concentration distribution.

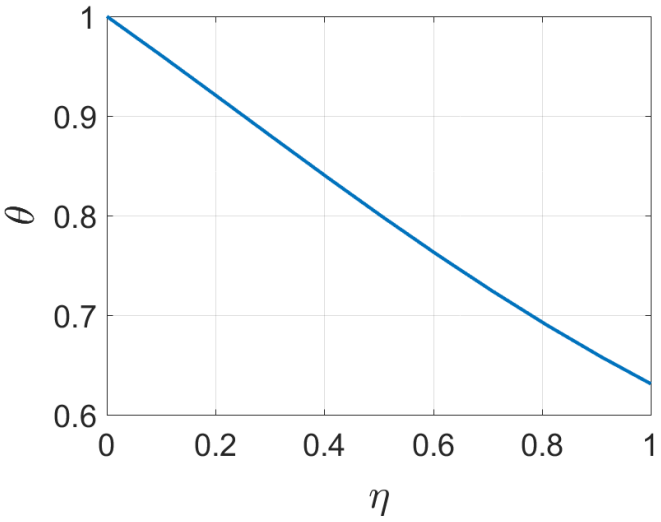


**Figure 4.** Temperature distribution.

The findings and their implications are summarized in Table 4, where all the important results, by different parameter, are presented. Table 4 explains the effect of radiation parameter, Prandtl number, Brinkmann number, non-Newtonian power index, Hartmann number, and volumetric heat generation on boundary later thickness and Nusselt number. Future research directions may also be done by considering Brownian motion effects and Soret effects. Boundary-layer characteristics in Table 4 are symbolized by parameter $\delta$. It is observed that for increasing values of Hartman number, the velocity and the boundary-layer thickness increase and decrease the temperature distribution. It could be understood by the curvature of the velocity and temperature profile. Specific results of the magnetic parameter on the chemical reaction at the boundary are plotted in Figures 5–7. As shown in Figure 5, the $\phi'$ function at the stretched wall decrease as the Hartmann increase. The Figure is a plot of results obtained for $N_b = 0$, $Q = 0$, $Pr = 1$, $Br = 1$, $\gamma = 1$, $Sc = 1$. Concentration distributions plotted in Figure 3 shows that inside the boundary layer the concentration decreases while the magnetic force makes the figure curvier and causes lower gradients in the stretched surface. This is because an increase in Hartmann number will increase the intensity of body force, which acts as a negative pressure gradient force near the stretching surface and hence tends to thicken the boundary layer. Furthermore, an increase of thermophoresis parameter in the medium decreases the boundary flux of concentration. Figure 6 reveals the concentration gradients at the moving wall versus the non-dimensional magnetic

parameter for various Brownian parameters. The Figure is a plot of results obtained for $N_t = 0$, $Q = 0$, $Pr = 1$, $Br = 1$, $\gamma = 1$, $Sc = 1$. It is observed that for increasing values of Hartmann number, the dimensionless concentration flux decreases, and the concentration boundary-layer thickness increases and decreases the concentration flux distribution near the wall. Furthermore, the increase of Brownian parameter in the medium decreases the boundary flux of concentration.

**Table 4.** Parameter effects on heat transfer and boundary-layer characteristics.

| | $\delta$ | $Nu$ |
|---|---|---|
| $n$ (0 to 1) | decrease | increase |
| $Pr$ (0.001 to 10) | decrease | increase |
| $N_R$ (0 to 2) | increase | decrease |
| $Br$ (0 to 10) | increase | increase |
| $Ha$ (0 to 1) | downward parabola | downward parabola |
| $Q_r$ (0 to 0.01) | downward parabola | downward parabola |

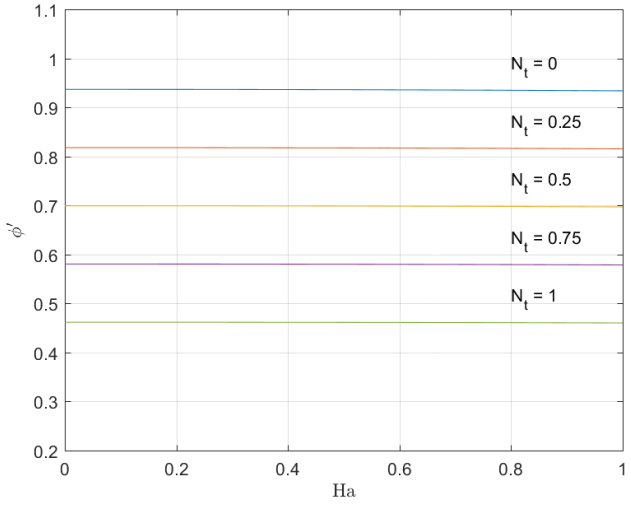


**Figure 5.** MHD and thermophoresis diffusion parameter effects on the rate of the chemical reaction in the boundary.

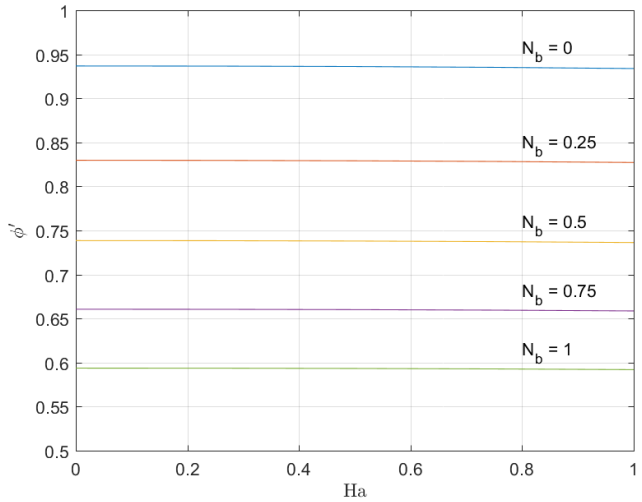


**Figure 6.** MHD and Brownian diffusion parameter effects on the rate of the chemical reaction in the boundary.

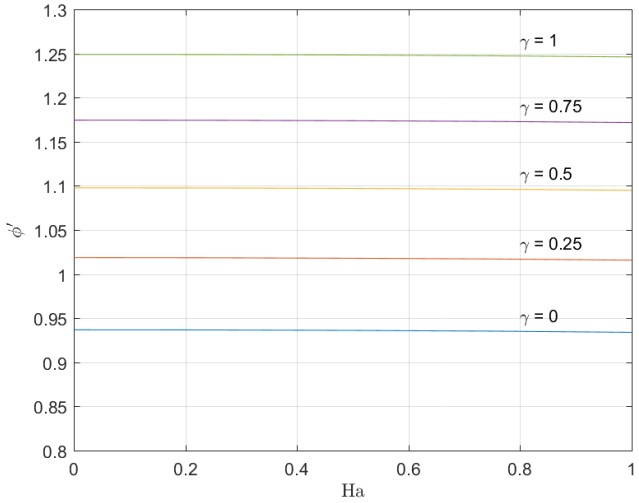


**Figure 7.** MHD and chemical reaction parameter effects on the rate of the chemical reaction in the boundary.

Figure 7 exposes the temperature distribution versus the non-dimensional distance. The Figure is a plot of results obtained for $N_b = 0, N_t = 0, Q = 0, Pr = 1, Br = 1, \gamma = 1, Sc = 1$. It is observed that for increasing values of Hartmann number, the dimensionless concentration gradients decrease and the concentration boundary-layer thickness increase and decrease the concentration flux distribution near the wall. Furthermore, the increase in chemical reaction parameter in the medium increase the boundary flux of concentration. The findings and their implications are summarized in Table 5 where all the important results, by different parameter, are presented.

**Table 5.** Parameters effects on the chemical reaction in the boundary.

| | $\delta_c$ | $\phi'$ |
|---|---|---|
| $N_t$ | increase | decrease |
| $N_b$ | increase | decrease |
| $\gamma$ | decrease | increase |

As the MHD affected the chemical reaction indirectly, its effect should be considered by the coupling with other parameters. Because the goal of the present article is to investigate the MHD effects in a steady-state fully developed incompressible flow over an axisymmetric stretching sheet, in Figures 5–7, the rate of the chemical reaction is released which is almost independent of MHD effect. The plots are given versus the MHD parameter instead of diffusion and reaction parameters to show the dominance of the chemical parameter over the MHD parameter. If just the MHD parameter changes over a broader range, the results here show the effect to be more visible, while in Figures 5–7 the importance is discussed for the base levels coming from chemical parameters.

## 4. Conclusions

The coupled problem of heat, fluid flow, and mass transfer through a chemical reactive medium is of importance in science and engineering application such as the dying industry, polymer industry, food industry, the metallurgy of metal plates, and have since received a high level of attention in recent times. Distribution of temperature, fluid motion and chemical components over a stretched sheet is useful in agricultural applications and groves of fruit trees, freezing problems of fruit, evaporation of the fruit water content at the surface of it and heat transfer at the cooling towers. The goal of the present article is to investigate the MHD effects in a steady-state fully developed incompressible flow over an axisymmetric stretching sheet; the rate of the chemical reaction is shown to have a minor effect

of MHD in low Hartmann numbers, since the MHD effect can be considered by the coupling with other parameters. The results show that the chemical reaction parameter has an increasing effect on the chemical reaction boundary while the magnetic, thermophoresis, and Brownian effects decrease the rate of the chemical reaction at the boundary.

**Funding:** This research received no external funding.

**Conflicts of Interest:** The author declares no conflict of interest.

## Abbreviations

The following abbreviations are used in this manuscript:

| | |
|---|---|
| MHD | Magneto Hydro Dynamics |

## Nomenclature

| | | |
|---|---|---|
| Be | local Bejan number | |
| *Br* | Brinkmann number | |
| $C_p$ | specific heat at constant pressure | J/kg·K |
| $D_B$ | Brownian diffusion coefficient | $m^2/s$ |
| $D_T$ | thermophoresis diffusion coefficient | $m^2/s$ |
| *Ha* | Harttmann number | |
| *k* | thermal conductivity of the fluid | W/mK |
| $k_1$ | chemical reaction coefficient | |
| K | flow consistency index | |
| *n* | power-law index | |
| *n** | refractive index | |
| $N_b$ | Brownian motion parameter | |
| $N_R$ | Radiative number | |
| $N_t$ | thermophoresis parameter | |
| *Q* | Heat source coefficient | |
| *r* | Coordinate component | m |
| *Pr* | Prantdl number | |
| *T* | medium temperature | K |
| $T_w$ | temperature of the fluid near wall | K |
| $T_\infty$ | temperature of the fluid near wall | K |
| *u* | velocity component in the zrdirection | m/s |
| *v* | velocity component in the r direction | m/s |
| *z* | Coordinate component | m |

## Greek Symbol

| | | |
|---|---|---|
| $\alpha$ | thermal diffusivity | $m^2/s$ |
| emph$\gamma$ | chemical reaction parameter | |
| $\theta$ | dimensionless temperature | |
| $\sigma$ | fluid electric conductivity | S/m |
| $\rho$ | fluid density | $kg/m^3$ |
| $\sigma^*$ | Stephan–Boltzman constant | $kg{\cdot}s^{-3}{\cdot}K^{-4}$ |
| $\chi$ | Rosseland-mean absorption coefficient | |
| $\mu$ | viscosity of the fluid | Pa·s |
| $\rho$Cp | heat capacitance | $J/m^3{\cdot}K$ |

## References


1. Crane, L.J. Flow past a stretching plate. *Z. Angew. Math. Phys.* **1970**, *21*, 645–647. [CrossRef]
2. Gupta, P.S.; Gupta, A.S. Heat and mass transfer on a stretching sheet with suction or blowing. *Can. J. Chem. Eng.* **1977**, *55*, 744–746. [CrossRef]
3. Grubka, J.; Bobba, K.M. Heat transfer characteristics of a continuous stretching surface with variable temperature. *J. Heat Transf.* **1985**, *107*, 248–250. [CrossRef]
4. Ali, M.E. On thermal boundary layer on a power law stretched surface with suction or injection. *Int. J. Heat Fluid Flow* **1995**, *16*, 280–290. [CrossRef]
5. Chen, C.H. Laminar mixed convection adjacent to vertical, continuously stretching sheets. *Heat Mass Transf.* **1998**, *33*, 471–476. [CrossRef]
6. Datta, B.K.; Roy, P.; Gupta, A.S. Temperature field in a flow over a stretching that within uniform heat flux. *Int. Commun. Heat Transf.* **1985**, *12*, 89–94. [CrossRef]
7. Chen, C.K.; Char, M.I. Heat transfer on a continuous stretching surface with suction or blowing. *J. Math. Anal. Appl.* **1988**, *135*, 568–580. [CrossRef]
8. Elbashbeshy, E.M.A. Heat transfer over a stretching surface with variable heat flux. *J. Phys. D Appl. Phys.* **1998**, *31*. [CrossRef]
9. Hooshmand, P.; Gatabi, H.; Bagheri, N.; Pirzadeh, I.I.; Hesabi, A.; Abdollahzadeh Jamalabadi, M.; Oveisi, M. Numerical study of the magnetic field effects on the heat transfer and entropy generation aspects of a power law fluid over an axisymmetric stretching plate structure. *Entropy* **2017**, *19*, 94. [CrossRef]
10. Abdollahzadeh Jamalabadi, M.Y. Entropy generation in boundary layer flow of a micro polar fluid over a stretching sheet embedded in a highly absorbing medium. *Front. Heat Mass Trans.* **2015**, *6*, 1–13. [CrossRef]
11. Cortell, R. Flow and heat transfer of a fluid through a porous medium over a stretching surface with internal heat generation/absorption and suction/blowing. *Fluid Dyn. Res.* **2005**, *37*, 231–245. [CrossRef]
12. Liao, S.J. An analytic solution of unsteady boundary-layer flows caused by an impulsively stretching plate. *Commun. Nonlinear Sci. Numer. Simul.* **2006**, *11*, 326–339. [CrossRef]
13. Mehmood, A.; Ali, A. Analytic homotopy solution of generalized three dimensional channel flow due to uniform stretching of the plate. *Acta Mech. Sin.* **2007**, *23*, 502–510. [CrossRef]
14. Ishak, A.; Nazar, R.; Pop, I. Hydromagnetic flow and heat transfer adjacent to a stretching vertical sheet. *Heat Mass Transf.* **2008**, *44*, 921–927. [CrossRef]
15. Crane, L.J. Boundary layer flow due to stretching cylinder. *Z. Angew. Math. Phys.* **1975**, *25*, 619–622. [CrossRef]
16. Wang, C.Y. Fluid flow due to stretching cylinder. *Phys. Fluids* **1988**, *31*, 466–468. [CrossRef]
17. Burde, H.I. On the motion of fluid near a stretching circular cylinder. *J. Appl. Math. Mech.* **1988**, *53*, 271–273. [CrossRef]
18. Ishak, A.; Nazar, R. Laminar boundary layer flow along a stretching cylinder. *Eur. J. Sci. Res.* **2009**, *36*, 22–29.
19. Ishak, A.; Nazar, R.; Pop, I. Magnetohydrodynamic (MHD) flow and heat transfer due to a stretching cylinder. *Energy Convers. Manag.* **2008**, *49*, 3265–3269. [CrossRef]
20. Mastroberardino, A.; Paullet, J.E. Existence and priori bounds for steady stagnation flow toward a stretching cylinder. *J. Math. Anal. Appl.* **2010**, *365*, 701–710. [CrossRef]
21. Weidman, P.D.; Ali, M.E. Aligned and nonaligned radial stagnation flow on a stretching cylinder. *Eur. J. Mech. B Fluids* **2011**, *30*, 120–128. [CrossRef]
22. Wang, C.Y.; Ng, C.O. Slip flow due to a stretching cylinder. *Int. J. Nonlinear Mech.* **2011**, *45*, 1191–1194. [CrossRef]
23. Munawar, S.; Mehmood, A.; Ali, A. Unsteady flow of viscous fluid over the vacillate stretching cylinder. *Int. J. Numer. Methods Fluids* **2011**, *70*, 671–681. [CrossRef]
24. Vajravelu, K.; Prasad, K.V.; Santhi, S.R. Axisymmetric magneto-hydrodynamic (MHD) flow and heat transfer at a non-isothermal stretching cylinder. *Appl. Math. Comput.* **2012**, *219*, 3993–4005. [CrossRef]
25. Jamalabadi, M.Y.A.; Park J.H. Thermal radiation, joule heating, and viscous dissipation effects on MHD forced convection flow with uniform surface temperature. *Open J. Fluid Dyn.* **2014**, *4*, 125–132. [CrossRef]
26. Jamalabadi, M.Y.A. EMHD effects on subcooled boiling in a Vertical annulus. *Multiph. Sci. Technol.* **2019**, *6*, 333–349. [CrossRef]
27. Jamalabadi, M.Y.A. Electromagnetohydrodynamic two-phase flow-induced vibrations in vertical heated upward flow. *J. Comput. Des. Eng.* **2019**, *6*, 92–104. [CrossRef]

28. Chen, X.; Pavlish, K.; Benoit, J.N. Myosin phosphorylation triggers actin polymerization in vascular smooth muscle. *Am. J. Physiol. Heart Circ. Physiol.* **2008**, *295*, H2172–H2177. [CrossRef] [PubMed]
29. Jones, E.A.V. The initiation of blood flow and flow induced events in early vascular development. *Semin. Cell Dev. Biol.* **2011**, *22*, 1028–1035. [CrossRef] [PubMed]
30. Das, A.; Paul, A.; Taylor, M.D.; Banerjee, R.K. Pulsatile arterial wall-blood flow interaction with wall pre-stress computed using an inverse algorithm. *Biomed. Eng. Online* **2015**, *14*, S1–S18. [CrossRef] [PubMed]
31. Blachon, A.; Marque, S.R.A.; Roubaud, V.; Siri, D. Diasteromeric Effect on the Homolysis of the C–ON Bond in Alkoxyamines: A DFT Investigation of 1,3-Diphenylbutyl-TEMPO. *Polymers* **2010**, *2*, 353–363. [CrossRef]
32. Yu, J.; Liu, F.; Tang, P.; Qiu, F.; Zhang, H.; Yang, Y. Effect of Geometrical Asymmetry on the Phase Behavior of Rod-Coil Diblock Copolymers. *Polymers* **2016**, *8*, 184. [CrossRef][PubMed]
33. Kogej, K. Thermodynamic Analysis of the Conformational Transition in Aqueous Solutions of Isotactic and Atactic Poly(Methacrylic Acid) and the Hydrophobic Effect. *Polymers* **2016**, *8*, 168. [CrossRef] [PubMed]
34. Odat, M.Q.A.; Damseh, R.A.; Nimr, M.A.A. Effect of magnetic field on entropy generation due to laminar forced convection past a horizontal flat plate. *Entropy* **2004**, *4*, 293–303. [CrossRef]
35. Makinde, O.D.; Osalusi, E. Entropy generation in a liquid film falling along an inclined porous heated plate. *Mech. Res. Commun.* **2006**, *33*, 692–698. [CrossRef]
36. Makinde, O.D. Irreversibility analysis for a gravity driven non-Newtonian liquid film along an inclined isothermal plate. *Phys. Scr.* **2006**, *74*, 642–645. [CrossRef]
37. Mukhopadhyay, S.; Ishak, A. Mixed convection flow along a stretching cylinder in a thermally stratified medium. *J. Appl. Math.* **2012**, *8*. [CrossRef]
38. Shateyi, S.; Marewo, G.T. A new numerical approach for the laminar boundary layer flow and heat transfer along a stretching cylinder embedded in a porous medium with variable thermal conductivity. *J. Appl. Math.* **2013**, *7*. [CrossRef]
39. Si, X.; Li, L.; Zheng, L.; Zhang, X.; Liu, B. The exterior unsteady viscous flow and heat transfer due to a porous expanding stretching cylinder. *Comput. Fluids* **2014**, *105*, 280–284. [CrossRef]
40. Vajravelu, K.; Prasad, K.V.; Santhi, S.R.; Umesh, V. Fluid flow and heat transfer over a permeable stretching cylinder. *J. Appl. Fluids Mech.* **2014**, *7*, 111–120.
41. Alharbi, S.; Dawar, A.; Shah, Z.; Khan, W.; Idrees, M.; Islam, S.; Khan, I. Entropy Generation in MHD Eyring–Powell Fluid Flow over an Unsteady Oscillatory Porous Stretching Surface under the Impact of Thermal Radiation and Heat Source/Sink. *Appl. Sci.* **2018**, *8*, 2588. [CrossRef]
42. Munawar, S.; Ali, A.; Mehmood, A. Thermal analysis of the flow over an oscillatory stretching cylinder. *Phys. Scr.* **2012**, *86*. [CrossRef]
43. Butt, A.S.; Ali, A. Entropy analysis of magnetohydrodynamic flow and heat transfer due to a stretching cylinder. *J. Taiwan Inst. Chem. Eng.* **2014**, *45*, 780–786. [CrossRef]
44. Osswald, T.; Baur, E.; Brinkmann, S.; Oberbach, K.; Schmachtenberg, E. *International Plastics Handbook 4E: The Resource for Plastics Engineers*, 4th ed.; Hanser Publications: Munich, Germany, 2006.
45. Brostow, W. *Mechanical and Thermophysical Properties of Polymer Liquid Crystals*; Chapman & Hall: New York, NY, USA, 1998; Volume 3.
46. Rosseland, S. *Theoretical Astrophysics: Atomic Theory and the Analysis of Stellar Atmospheres and Envelopes*; Clarendon Press: Oxford, UK, 1936.
47. Press, W.H.; Teukolsky, S.A.; Vetterling, W.T.; Flannery, B.P. *Numerical Recipes: The Art of Scientific Computing*; Cambridge University Press: New York, NY, USA, 2007.
48. Makinde, O.D.; Mabood, F.; Khanc, W.A.; Tshehla, M.S. MHD flow of a variable viscosity nanofluid over a radially stretching convective surface with radiative heat. *J. Mol. Liq.* **2016**, *219*, 624–630. [CrossRef]
49. Motsa, S.S.; Sibanda, P. On the solution of MHD flow over a nonlinear stretching sheet by an efficient semi-analytical technique. *Int. J. Numer. Methods Fluids* **2012**, *68*, 1524–1537. [CrossRef]
50. Abdollahzadeh Jamalabadi, M.Y.; Hooshmand, P.; Bagheri, N.; KhakRah, H.; Dousti, M. Numerical Simulation of Williamson Combined Natural and Forced Convective Fluid Flow between Parallel Vertical Walls with Slip Effects and Radiative Heat Transfer in a Porous Medium. *Entropy* **2016**, *18*, 147. [CrossRef]
51. Khan, M.; Munir, A.; Shahzad, A. Convective Heat Transfer to Sisko Fluid over a Nonlinear Radially Stretching Sheet. In *Heat Transfer Studies and Applications*; Kazi, S.N., Ed.; Intech: Rijeka, Croatia, 2015; pp. 341–361.

52. Drikakis, D.; Asproulis, N. Multiscale Computational Modelling of Flow and Heat Transfer. *Int. J. Numer. Method Heat Fluid Flow* **2010**, *20*, 517–528. [CrossRef]
53. Asproulis, N.; Kalweit, M.; Drikakis, D. A hybrid molecular continuum method using point wise coupling. *Adv. Eng. Softw.* **2012**, *46*, 85–92. [CrossRef]
54. Kalweit, M.; Drikakis, D. Coupling strategies for hybrid molecular—Continuum simulation methods. *Proc. IMechE Part C* **2008**, *222*, 797–806. [CrossRef]
55. Di Federico, V.; Archetti, R.; Longo, S. Spreading of axisymmetric non-Newtonian power-law gravity currents in porous media. *J. Non-Newton. Fluid Mech.* **2012**, *189–190*, 31–39. [CrossRef]
56. De Haro, M.L.; Cuevas, S.; Beltran, A. Heat transfer and entropy generation in the parallel plate flow of a power-law fluid with asymmetric convective cooling. *Energy* **2014**, *66*, 750–756. [CrossRef]
57. Anand, V. Slip law effects on heat transfer and entropy generation of pressure driven flow of a power law fluid in a microchannel under uniform heat flux boundary condition. *Energy* **2014**, *76*, 716–732. [CrossRef]
58. Sheremet, M.A.; Oztop, H.F.; Pop, I.; Abu-Hamdeh, N. Analysis of entropy generation in natural convection of nanofluid inside a square cavity having hot solid block: Tiwari and Das' model. *Entropy* **2016**, *18*, 9. [CrossRef]
59. Pascal, J.P.; Pascal, H. Similarity solutions to gravity flows of non-Newtonian fluids through porous media. *Int. J. Non-Linear Mech.* **1993**, *28*, 157–167. [CrossRef]
60. Chowdhury, M.R.; Testik, F.Y. Viscous propagation of two-dimensional non-Newtonian gravity currents. *Fluid Dyn. Res.* **2012**, *44*, 4. [CrossRef]
61. Tosco, T.; Sethi, R. Transport of Non-Newtonian Suspensions of Highly Concentrated Micro- and Nanoscale Iron Particles in Porous Media: A Modeling Approach. *Environ. Sci. Technol.* **2010**, *44*, 9062–9068. [CrossRef] [PubMed]
62. Ciriello, V.; Longo, S.; Di Federico, V. On shear thinning fluid flow induced by continuous mass injection in porous media with variable conductivity. *Mech. Res. Commun.* **2013**, *52*, 101–107. [CrossRef]
63. Longo, S.; Di Federico, V.; Chiapponi, L.; Archetti, R. Experimental verification of power-law non-Newtonian axisymmetric porous gravity currents. *J. Fluid Mech.* **2013**, *731*. [CrossRef]
64. Longo, S.; di Federico, V.; Archetti, R.; Chiapponi, L.; Ciriello, V.; Ungarish, M. On the axisymmetric spreading of non-Newtonian power-law gravity currents of time-dependent volume: An experimental and theoretical investigation focused on the inference of rheological parameters. *J. Non-Newton. Fluid Mech.* **2013**, *201*, 69–79. [CrossRef]
65. Di Federico, V.; Longo, S.; Chiapponi, L.; Archetti, R.; Ciriello, V. Radial gravity currents in vertically graded porous media: Theory and experiments for Newtonian and power-law fluids. *Adv. Water Resour.* **2014**, *70*, 65–76. [CrossRef]
66. Longo, S.; Di Federic, V.; Chiapponi, L. Non-Newtonian power-law gravity currents propagating in confining boundaries. *Environ. Fluid Mech.* **2015**, *15*, 515–535. [CrossRef]
67. Longo, S.; Ciriello, V.; Chiapponi, L.; Di Federico, V. Combined effect of rheology and confining boundaries on spreading of gravity currents in porous media. *Adv. Water Resour.* **2015**, *79*, 140–152. [CrossRef]
68. Longo, S.; Di Federico, V.; Chiapponi, L. Propagation of viscous gravity currents inside confining boundaries: The effects of fluid rheology and channel geometry. *Proc. R. Soc. A Math. Phys. Eng. Sci.* **2015**. [CrossRef]
69. Longo, S.; Di Federico, V. Stability Analysis of Gravity Currents of a Power-Law Fluid in a Porous Medium. *Math. Probl. Eng.* **2015**, *2015*, 286487. [CrossRef]
70. Longo, S.; Di Federico, V.; Chiapponi, L. A dipole solution for power-law gravity currents in porous formations. *J. Fluid Mech.* **2015**, *778*, 534–551. [CrossRef] [CrossRef]
71. Longo, S.; Di Federico, V. Unsteady Flow of Shear-Thinning Fluids in Porous Media with Pressure-Dependent Properties. *Transp. Porous Med.* **2015**, *110*, 429–447. [CrossRef]
72. Ciriello, V.; Longo, S.; Chiapponi, L.; Di Federico, V. Porous gravity currents: A survey to determine the joint influence of fluid rheology and variations of medium properties. *Adv. Water Resour.* **2016**, *92*, 105–115. [CrossRef]
73. Longo, S.; Chiapponi, L.; di Federico, V. On the propagation of viscous gravity currents of non-Newtonian fluids in channels with varying cross section and inclination. *J. Non-Newton. Fluid Mech.* **2016**, *235*, 95–108. [CrossRef]

74. Hayat, T.; Khan, M.I.; Farooq, M.; Alsaedi, A.; Waqas, M.; Yasmeen, T. Impact of Cattaneo-Christov heat flux model in flow of variable thermal conductivity fluid over a variable thicked surface. *Int. J. Heat Mass Transf.* **2016**, *99*, 702–710. [CrossRef]
75. Khan, M.I.; Waqas, M.; Hayat, T.; Alsaedi, A. A comparative study of Casson fluid with homogeneous-heterogeneous reactions. *J. Colloid Interface Sci.* **2017** , *498*, 85–90 [CrossRef]
76. Hayat, T.; Khan, M.I.; Qayyum, S.; Alsaedi A. Entropy generation in flow with silver and copper nanoparticles. *Colloids Surf. A Physicochem. Eng. Asp.* **2018**, *539*, 335–346, [CrossRef]
77. Khan, M.I.; Waqas, M.; Hayat, T.; Alsaedi, A.; Khan, M.I. Significance of nonlinear radiation in mixed convection flow of magneto Walter-B nanoliquid. *Int. J. Hydrog. Energy* **2017**, *42*, 26408–26416 [CrossRef]
78. Rashid, M.; Khan, M.I.; Hayat, T.; Khan, M.I.; Alsaedi, A. Entropy generation in flow of ferromagnetic liquid with nonlinear radiation and slip condition. *J. Mol. Liq.* **2019**, *276*, 441–452 [CrossRef]